

# Chemical vapour deposition of silicon nitride in a microwave plasma assisted reactor

O. R. MONTEIRO, ZHI WANG, I. G. BROWN

Lawrence Berkeley National Laboratory, University of California, Berkeley, CA 94720 USA

Microwave plasma assisted chemical vapour deposition was used to produce silicon nitride films on silicon substrates from mixtures of methane and nitrogen. Deposition temperatures varied from 800 to 1000 °C and pressure varied from 53.2 to  $79.8 \times 10^2$  Pa. Gas mixtures with low methane content resulted in no reaction. Gas mixtures with high methane content produced an amorphous carbon film on the silicon wafer surface. At intermediate methane contents, the process produces a mixture of  $\alpha$  and  $\beta$  silicon nitride. A mechanism is proposed according to which the silicon surface is chemically etched by the activated methyl radicals forming  $\text{Si}(\text{CH}_3)_4$ , which then reacts with nitrogen atoms (or ions) to form the silicon nitride. The morphology of the individual crystals evolves from platelets to needle-like depending on the deposition conditions, and on the surface coverage of the silicon surface.

## 1. Introduction

Several methods have been used for producing crystalline and amorphous silicon nitride films starting from a variety of gas mixtures. Plasma assisted processes are commonly used to manufacture amorphous silicon nitride for the electronics industry. The main applications in this industry are as final passivation and mechanical protective layers for integrated circuits, as masks for selective oxidation of silicon, and as gate dielectric material in metal–nitride–oxide semiconductor (MNOS) devices [1]. High temperature chemical vapour deposition (CVD) is sometimes utilized to produce crystalline films, although the high temperature requirements (over 900 °C) hinder its application in electronic materials processing [2]. The mechanical and chemical properties of this material, however, make it usable in a variety of other engineering applications. Other methods that have been proposed for the production of silicon nitride powders, include carbothermic reduction of silicon dioxide [3, 4] and direct nitriding of silicon powders [5, 6].

The use of microwave produced plasmas for nitriding a variety of material surfaces has increased in the last few years [7, 8]. The formation of crystalline silicon nitride thin films using microwave plasma enhanced CVD has been studied by Grannen *et al.* [9]. In this study, deposition was accomplished from plasma prepared from a mixture of an organo-silicon gas with nitrogen in one case, or simply by exposing the silicon substrate to a nitrogen/methane plasma.

Here, we present our results on the microwave plasma assisted synthesis of silicon nitride films, and discuss our findings in light of the published literature. Particular emphasis is given to understanding the reaction mechanism, growth morphologies, and characterization of the reaction products. A discussion of

the effect of deposition conditions of the process is also provided.

## 2. Experimental procedure

The microwave system utilized in this work is described elsewhere [10], and was originally constructed for our studies on diamond synthesis. A 2.45 GHz, 700 W magnetron produces the microwave power that ionizes the gas stream inside a quartz bell-jar reaction chamber, forming a plasma ball directly above the surface of a heated substrate. Temperature of the back side of the substrate is measured using a two-colour IR pyrometer directly pointed at it. Due to the small thicknesses of the silicon wafers used in these experiments, as well as the long deposition times, we assume that the temperature is uniform throughout the wafer.

Experiments were conducted using two different gas mixtures:  $\text{N}_2$  and  $\text{CH}_4$ , and  $\text{N}_2$  and  $\text{H}_2$ . In the former case, flow rates of  $\text{N}_2$  and  $\text{CH}_4$  were varied from 100 sccm (standard cubic centimeters per minute) to 300 sccm and 1 sccm to 3 sccm, respectively. In the latter set of experiments, flow rates of  $\text{N}_2$  and  $\text{H}_2$  varied from 100 sccm to 300 sccm and 5 sccm to 20 sccm, respectively. Experiments with pure nitrogen were also attempted in order to understand the reaction mechanism. (1 1 1) and (1 0 0) silicon substrates 2.5 cm diameter were used for the synthesis of silicon nitride. The substrate was placed on a quartz pedestal inside the bell-jar, just underneath the plasma ball. Gas flow rates and composition ratios in the gas stream were varied to evaluate their effect on the film formation.

The experimental conditions used for the deposition of  $\text{Si}_3\text{N}_4$  using methane and nitrogen as the plasma forming gas are given in Table I. Table II lists the conditions used when hydrogen–nitrogen mixtures were used.

TABLE I Experimental conditions for MWPACVD of silicon nitride using  $\text{CH}_4:\text{N}_2$

Substrate	Si (1 1 0) or Si (1 1 1)
Time	1–15 h
Methane flowrate	1–5 sccm
Nitrogen flowrate	50–300 sccm
Microwave power	700 W
Pressure	40–60 T
Temperature	800–1000 °C

TABLE II Experimental conditions for MWPACVD of silicon nitride using  $\text{H}_2:\text{N}_2$

Substrate	Si (1 1 0) or Si (1 1 1)
Time	1–15 h
Hydrogen flowrate	5–20 sccm
Nitrogen flowrate	50–300 sccm
Microwave power	700 W
Pressure	40–60 T
Temperature	800–1000 °C

Film characterization was conducted by several techniques. Grazing-angle X-ray diffraction was done in a siemens D5000 diffractometer, with the objective of determining the phases present, as well as the crystallinity of the films.  $\text{CuK}_\alpha$  radiation was used to obtain the diffractograms. The scan step size was  $0.02^\circ$ , incidence angle  $1^\circ$ , and the scanning range was 20 to  $65^\circ$ . Scanning electron microscopy (SEM) was used to observe the morphology of the film, with a Jeol 6400 SEM at operating voltage of 30 kV. Transmission electron microscopy (TEM) was used to further characterize the microstructure of the film. TEM work was conducted on a Jeol 200CX with a resolution of 0.23 nm at 200 kV. Samples for TEM were prepared for planar view as well as cross-section observations. In both cases dimpling followed by ion-milling at liquid nitrogen temperature was the method utilized. Cross-section electron microscopy was also used to analyse the interface, and any variation of film microstructure with depth.

### 3. Results

Among the experimental conditions utilized in this study, formation of  $\text{Si}_3\text{N}_4$  only occurred when methane–nitrogen mixtures were used in the gas phase. Attempts to form  $\text{Si}_3\text{N}_4$  using the conditions described in Table II failed, i.e. mixtures of hydrogen and nitrogen resulted in no noticeable reaction at the silicon surface. No etching of the Si was observed under these conditions. An experiment in which the substrate was exposed to an  $\text{H}_2$  plasma at 900 °C for 2 h prior to the introduction of nitrogen also failed to produce any detectable amounts of  $\text{Si}_3\text{N}_4$ .

The results of the deposition experiments are summarized as follows. Methane lean  $\text{CH}_4:\text{N}_2$  mixtures (i.e. less than 1 : 300) resulted in no detectable  $\text{Si}_3\text{N}_4$ , for  $\text{CH}_4:\text{N}_2$  ratios between 1 : 300 and 1 : 50, silicon nitride deposition occurred concurrently with noticeable Si etching. For ratios greater than 1 : 50, amorphous carbon was the main product of the reaction,

which then formed a film on the silicon wafer, creating a barrier between its surface and the gas phase.

The surface morphology of the silicon nitride films is shown in Fig. 1, where we show scanning electron micrographs of the film after deposition for 15 h, with the  $\text{CH}_4:\text{N}_2$  ratio of 1 : 200. Fig. 1a shows an area in which the individual silicon nitride particles have not yet coalesced into a film. Several hexagonal platelets and needles can be seen on the Si surface. One immediate observation from this micrograph is the extensive etching of the substrate, which, as will be discussed later, is the source of Si for the nitride formation. In Fig. 1b, a partially coalesced  $\text{Si}_3\text{N}_4$  film is seen. The  $\text{Si}_3\text{N}_4$  crystals tend to be prismatic needles with hexagonal base. The transformation from platelet to needle-like morphology in growth from the vapour phase can be associated with a decrease in the degree of supersaturation, i.e. mixtures with greater degree of supersaturation lead to preferential platelet morphology, and those with lower degree of supersaturation result in needles. As we will point out in Section 4, this can be explained, based on the reaction mechanism proposed.

We found no difference in the film microstructure between depositions on (1 0 0) Si and (1 1 1) Si substrates. Both orientations showed etching patterns that

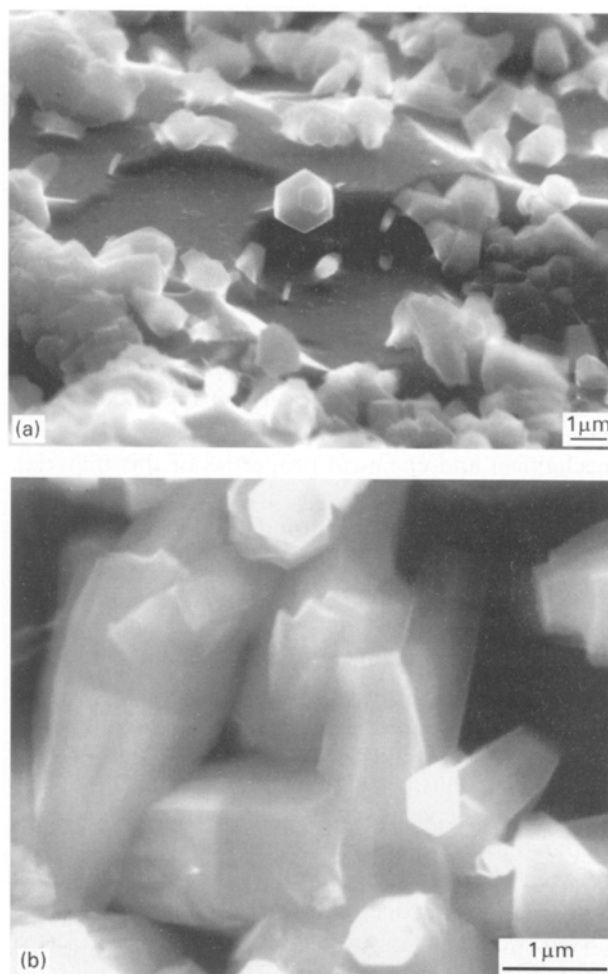


Figure 1 (a) Scanning electron micrograph of a sparsely coated silicon substrate after deposition with  $\text{CH}_4:\text{N}_2$  composition of 1 sccm: 200 sccm at 900 °C. (b) Scanning electron micrograph of silicon nitride film showing faceted needle-like crystals.

could not be directly related to any crystallographic planes. Severe etching resulted in a very rough interface between the Si and the  $\text{Si}_3\text{N}_4$ , as shown in Fig. 2. No predominant crystallographic relationship between the  $\text{Si}_3\text{N}_4$  and the Si substrate was observed, and the former seems to form in random orientations relative to the Si.

X-ray diffraction of the  $\text{Si}_3\text{N}_4$  films prepared from  $\text{CH}_4:\text{N}_2$  gas mixtures with ratios between 1:300 and 1:50 indicated that these films consisted primarily of  $\alpha$ - and  $\beta$ - $\text{Si}_3\text{N}_4$ . Contrary to the work of Grannen *et al.*, no tetragonal  $\text{Si}_3\text{N}_4$  was detected. Fig. 3 shows a typical X-ray diffractogram obtained from a film grown with a  $\text{CH}_4:\text{N}_2$  ratio of 1:200. Although no quantitative analysis was conducted, the predominant phase was the  $\alpha$ - $\text{Si}_3\text{N}_4$ , which is consistent with the fact that  $\beta$  phase is more stable at high temperatures, i.e. above 1400 °C, and the  $\alpha$  phase is more stable at low temperatures.

Analysis of transmission electron diffraction patterns of randomly selected grains in the  $\text{Si}_3\text{N}_4$  film also indicated that the films consisted of mixtures of the hexagonal  $\alpha$  and  $\beta$ - $\text{Si}_3\text{N}_4$  with the former in great quantity. Fig. 4 shows a bright field image of a plan view specimen prepared from a  $\text{Si}_3\text{N}_4$  film. Several of the grains in the film appear to have second phase inclusions, as marked in Fig. 4. The precise nature of

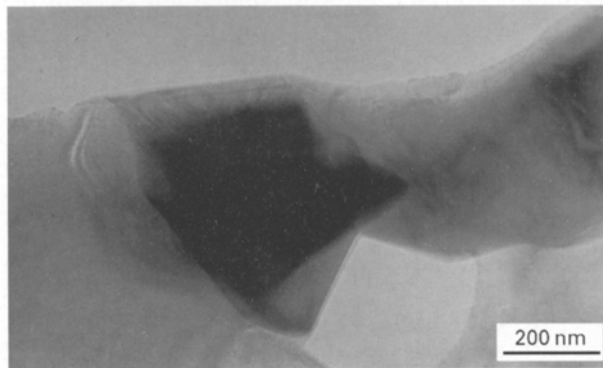


Figure 2 Cross-section transmission electron micrograph of the Si/ $\text{Si}_3\text{N}_4$  interface. Silicon is at the lower part of the print whereas the silicon nitride appears in darker contrast.

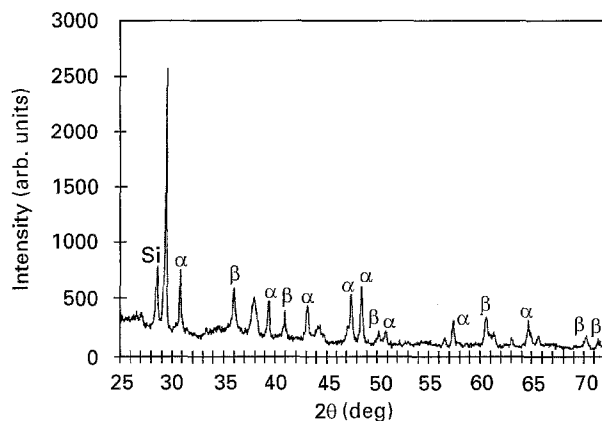


Figure 3 X-ray diffraction pattern of a silicon nitride film deposited with  $\text{CH}_4:\text{N}_2$  ratio of 1:200 at 900 °C.

such inclusions has not been determined yet. At least in some cases, electron diffraction has indicated that these inclusions consist of the  $\beta$ - $\text{Si}_3\text{N}_4$ . This does not exclude the possibility that the  $\beta$  phase could exist as isolated grains in the film, and in fact evidence from electron diffraction does suggest so. Inclusions in  $\alpha$ - $\text{Si}_3\text{N}_4$  may account for the spiral growth frequently observed in these films, as it will be discussed in the next section.

Mechanical abrasion of the substrate has a strong effect on the nucleation of  $\text{Si}_3\text{N}_4$  crystals, as shown in Fig. 5. One can see that the crystals have nucleated along a scratch mark on the substrate, whereas no  $\text{Si}_3\text{N}_4$  is found elsewhere around the scratch. No difference was observed in the etching characteristics of the substrate between regions near scratch marks and other regions on the substrate.

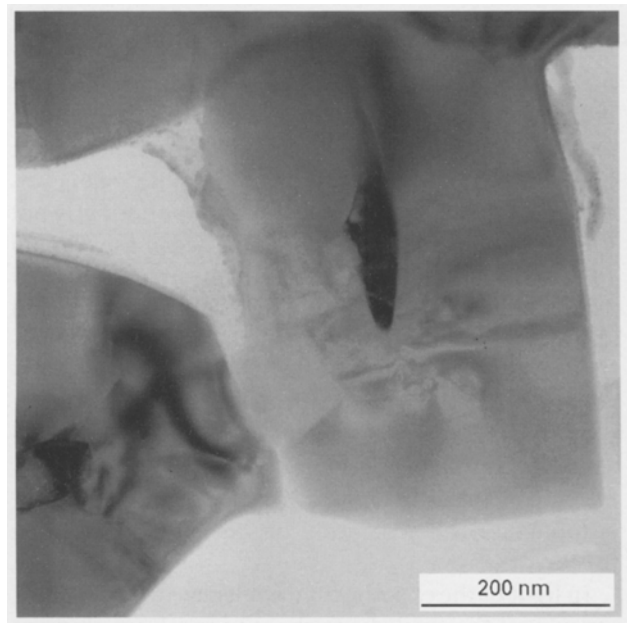


Figure 4 Bright field image of a plan view thin foil of silicon nitride film showing inclusions in the grains.

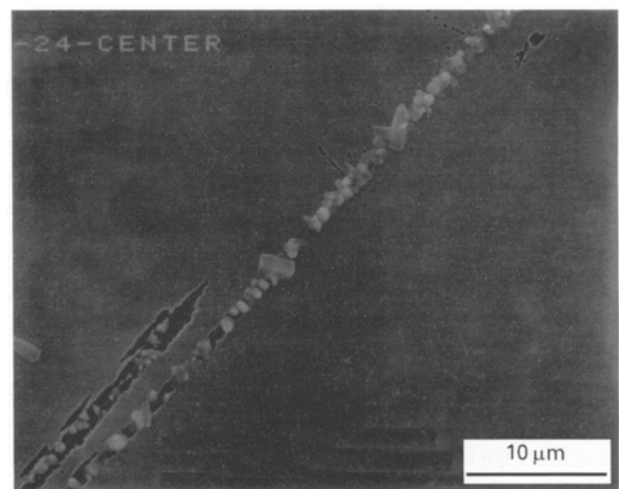


Figure 5 Scanning electron micrograph of a silicon substrate after growth for 5 h. Notice nucleation enhancement due to scratches in the silicon.

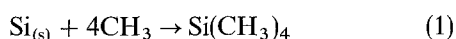
## 4. Discussion

### 4.1. Reaction mechanisms

The first issue that needs to be addressed is the source of silicon for the nitride formation. Grannen *et al.* [9] pointed out that  $\text{CH}_4$  in the gas phase is essential in order to form a volatile silicon-containing species, namely  $\text{Si}(\text{CH}_3)_4$ , which then reacts with nitrogen to form silicon nitride. We have unsuccessfully attempted to make  $\text{Si}_3\text{N}_4$  from reacting the silicon wafer with the microwave activated nitrogen plasma. Pre-treatment of the substrate at high temperature in a microwave-excited hydrogen plasma followed by exposure of the substrate to a mixture of activated nitrogen and hydrogen was also unsuccessful.

According to the mechanism proposed by Grannen *et al.* [9], silicon atoms are sputtered by nitrogen ions from the surface of the wafer, and once in the gas phase react with the methyl radicals to form  $\text{Si}(\text{CH}_3)_4$ . Critical evaluation of our experimental results suggests that the transfer of Si into the gas phase should result from a chemical rather than a purely physical effect. If sputtering of Si by N ions is the primary mechanism of forming Si atoms in the gas phase, it is difficult to explain the lack of reaction with a plasma gas mixture consisting of  $\text{N}_2$  and  $\text{H}_2$ . Moreover, under these conditions no surface damage to the wafers was observed, which again suggests that sputtering is not the main source of the silicon in the gas phase. Should silicon sputtering be of great significance, we could expect the presence of  $\text{SiH}_x$  in the gas phase, and according to the phase diagrams calculated by Lartigue *et al.* [11] silicon nitride would then be produced. The absence of silicon nitride when  $\text{N}_2$  and  $\text{H}_2$  are used and its presence when  $\text{N}_2$  and  $\text{CH}_4$  are used suggests that a chemical effect that requires the presence of methyl radicals, rather than a physical one, accounts for the generation of the silicon containing precursors.

In light of the experimental evidence presented here, we suggest that a likely mechanism for the microwave plasma assisted formation of silicon nitride can be described by Reactions 1 and 2 as follows

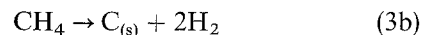


where the subscript (s) indicates that the species are in the solid state. Etching of silicon by methyl radicals generated in the plasma results in the formation of  $\text{Si}(\text{CH}_3)_4$ , which then reacts with excited nitrogen resulting in the deposition of crystalline silicon nitride.

This model is somewhat similar to Grannen's, although it differs in two main points: the nature of the process for carrying Si atoms into the gas phase, and the type of reactive species in the  $\text{CH}_4:\text{N}_2$  plasma that accounts for the silicon etching. According to the mechanism proposed here, the presence of  $\text{CH}_4$  in the gas mixture is not sufficient to produce  $\text{Si}(\text{CH}_3)_4$ . We have conducted experiments in the absence of the plasma, and observed no etching under this condition. Therefore it is the product(s) of the excitation of methane that accounts for the etching of Si. No attempt has

been made at this point to determine the concentration of the different activated species in the plasma.

As mentioned in the previous section, when the methane to nitrogen ratio exceeds 1:50, the primary product is amorphous carbon. Its deposition results primarily from the decomposition of the carbon containing species in the plasma, such as  $\text{CH}_3$  and  $\text{CH}_4$  according to



The carbon film acts as a physical barrier for further etching of silicon, preventing the formation of  $\text{Si}(\text{CH}_3)_4$  by Reaction 1, and therefore stopping the silicon nitride deposition. Fig. 6 shows an example of the competition between the deposition of an amorphous carbon film and the formation of silicon nitride. The crater where silicon nitride is still seen is surrounded by a much thicker a:C film, which isolates the gas phase from the silicon wafer.

### 4.2. Crystal Morphology

As can be seen in the scanning electron micrographs shown in Fig. 1, the silicon nitride film is made of, at least partially, well faceted needle-like hexagonal-base grains. Such morphology is consistent with the space groups  $\text{P}6_3/\text{m}$  and  $\text{P}31\text{c}$  of  $\beta$  and  $\alpha$ - $\text{Si}_3\text{N}_4$  respectively. In impeded crystal growth, equilibrium faces of the crystal, which are those having the lowest surface energy, tend to form the boundaries of the individual grains. Such faces are usually those of low Miller indices and with a high density of atomic packing.

At the early stages of the deposition with lean  $\text{CH}_4$  mixtures, the predominant morphology of the crystallites is platelike. The change in morphology from platelet to needle-like that occurs as the deposition proceeds can also be explained by the proposed growth mechanism described in Reactions 1 and 2. At the early stages of growth, there is a very large area of the Si substrate being etched, and therefore the amount of  $\text{Si}(\text{CH}_3)_4$  in the gas phase is large in comparison to later in the deposition. In this case the supersaturation for Reaction 2 is larger, and platelets



Figure 6 Scanning electron micrograph of an amorphous carbon film with a pin-hole in which silicon nitride can still be seen.

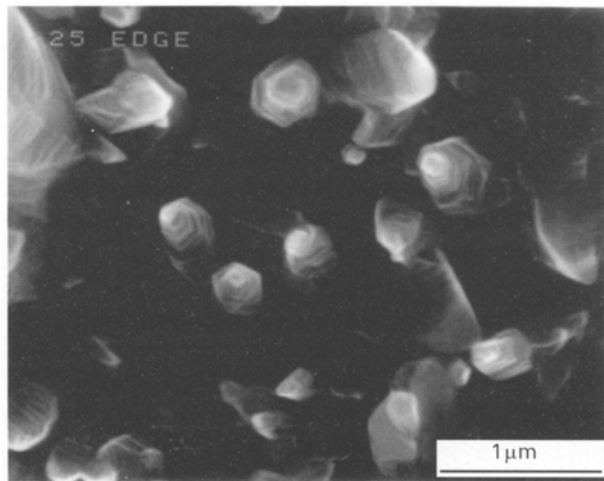


Figure 7 High magnification scanning electron micrograph showing spiral growth in silicon nitride crystals.

are more favourable to form. As deposition takes place, the surface area of Si available for etching decreases, and so does the concentration of  $\text{Si}(\text{CH}_3)_4$  in the gas phase, as well as the supersaturation. In this case a needle-like morphology predominates.

In this particular system, spiral growth as shown in Fig. 7 was often observed. An explanation for this type of growth was proposed by Frank [12], who first drew attention to the importance of screw dislocation in crystal growth processes. The spirals seen in Fig. 7 are in fact "macrospirals", with step height substantially greater than the unit cell. Amelinckx *et al.* [13] originally explained the existence of such steps as due to bunching of atomic dimension steps caused by some periodic fluctuation in the source of the microscopic spiral. Recently Zangwill [14] has presented some calculations that indicated the greater stability of adatoms in edges of terraces, which may lead to a thermodynamic explanation for the bunching of steps. Spiral growth as well as perfectly faceted crystal growth usually takes place under conditions of low supersaturation, i.e. close to equilibrium.

## 5. Conclusions

We have produced crystalline films of silicon nitride from an activated mixture of methane and nitrogen on a silicon wafer in a microwave plasma assisted reactor. The deposition process can be described by a chemical etching of the substrate forming silicon-containing

species in the gas phase, which then react with nitrogen to deposit as silicon nitride. The presence of methane in the gas phase is required in order to effectively produce the precursor for the nitride deposition, believed to be  $\text{Si}(\text{CH}_3)_4$ . The reaction product consists of a combination of  $\alpha$ - and  $\beta$ - $\text{Si}_3\text{N}_4$  with the former as the predominant phase. Inclusions in the  $\alpha$ - $\text{Si}_3\text{N}_4$  apparently account for promoting the spiral growth, frequently observed in this system.

## Acknowledgements

This work was supported by the Director, Office of Basic Energy Sciences, Advanced Energy Projects Division of the US Department of Energy under Contract No. DE-AC03-76SF00098. We would also like to acknowledge the support and use of the facilities of the National Center for Electron Microscopy at the Lawrence Berkeley National Laboratory, Berkeley CA.

## References

1. S. WOLF and R. N. TAUBER, "Silicon processing for the VLSI era" (Lattice Press, San Jose, CA, 1987).
2. S. MOTOJIMA, N. IWAMORI, T. HATTORI, *J. Mater. Sci.* **21** (1986) 3836.
3. M. EKELUND and B. FORSLUND, *J. Mater. Chem.* **2** (1992) 1079.
4. S. J. P. DURHAN, K. SHANKER and R. A. L. DREW, *J. Amer. Ceram. Soc.* **75** (1992) 532.
5. K. ISHIZAKI, S. YUMOTO and K. TAKANA, *J. Mater. Sci.* **23** (1988) 1813.
6. B. W. JONG, G. J. SLAVENS and D. E. TRAUT, *ibid.* **27** (1992) 6086.
7. H. MALVOS, A. RICARD, J. SZEKELY, H. MITCHEL, M. GANTOIS and D. ABLITZER, *Surface and Coatings Technol.* **59** (1993) 59.
8. A. RICARD, J. DESCHAMPS, J. L. GODARD, L. FALK and H. MICHEL, *Mater. Sci. Engng.* **A139** (1991) 9.
9. K. J. GRANNEN, F. XIONG and R. P. H. CHANG, *J. Mater. Res.* **9** (1994) 2341.
10. M. A. BREWER, I. G. BROWN, M. R. DICKINSON, J. E. GALVIN, R. A. MACGILL and M. C. SALVADORI, *Rev. Sci. Instrum.* **63** (1992) 3389.
11. J. F. LARTIGUE, M. DUCARRIOR, B. ARMAS, *J. Mater. Sci.* **19** (1984) 3079.
12. F. C. FRANK, *Disc. Faraday Soc.* **5** (1949) 48.
13. S. AMELINCKX, W. BONTINCK and W. DEKEYSER, *Phil. Mag.* **2** (1957) 1264.
14. A. ZANGWILL, Seminar presented at Lawrence Berkeley Laboratory, Spring 1995.

Received 18 December 1995  
and accepted 13 June 1996